Check for updates

Geophysical Research Letters

RESEARCH LETTER
10.1029/2023GL102879

How Does Tropical Cyclone Genesis Frequency Respond to a Changing Climate?

Jiuwei Zhao[1,2], Fang Wang[1], Ruifen Zhan[2,3], Yipeng Guo[4], Xin Huang[5,6], and Chao Liu[7]

[1]Collaborative Innovation Center on Forecast and Evaluation of Meteorological Disasters (CIC-FEMD), Institute of Climate and Application Research (ICAR), Nanjing University of Information Science & Technology (NUIST), Nanjing, China, [2]Department of Atmospheric and Oceanic Sciences, Fudan University, Shanghai, China, [3]Shanghai Frontiers Science Center of Atmosphere-Ocean Interaction, Fudan University, Shanghai, China, [4]School of Atmospheric Sciences, Nanjing University, Nanjing, China, [5]Shanghai Typhoon Institute, China Meteorological Administration, Shanghai, China, [6]Asia-Pacific Typhoon Collaborative Research Center, Shanghai, China, [7]Department of Atmospheric Sciences, Irreversible Climate Change Research Center, Yonsei University, Seoul, Korea

Key Points:

- The global tropical cyclone (TC) genesis frequency (TCGF) in response to uniform sea surface temperature (SST) changes shows a parabolic relation with a peak under 5 K-cooler climate than current climate
- The parabolic relation was found in all TC basins except the eastern North Pacific where the TCGF keeps increasing with SST changes
- Such a parabolic relation was attributed to the change in TC seed frequency

Supporting Information:

Supporting Information may be found in the online version of this article.

Correspondence to:

R. Zhan,
zhanrf@fudan.edu.cn

Citation:

Zhao, J., Wang, F., Zhan, R., Guo, Y., Huang, X., & Liu, C. (2023). How does tropical cyclone genesis frequency respond to a changing climate? *Geophysical Research Letters*, *50*, e2023GL102879. https://doi.org/10.1029/2023GL102879

Received 20 JAN 2023
Accepted 15 APR 2023

Author Contributions:

Conceptualization: Jiuwei Zhao
Data curation: Jiuwei Zhao, Xin Huang
Formal analysis: Jiuwei Zhao, Ruifen Zhan
Investigation: Jiuwei Zhao
Methodology: Jiuwei Zhao, Fang Wang, Yipeng Guo, Chao Liu
Software: Jiuwei Zhao, Fang Wang
Supervision: Ruifen Zhan
Visualization: Fang Wang
Writing – original draft: Jiuwei Zhao

© 2023. The Authors.
This is an open access article under the terms of the Creative Commons Attribution-NonCommercial-NoDerivs License, which permits use and distribution in any medium, provided the original work is properly cited, the use is non-commercial and no modifications or adaptations are made.

Abstract Global tropical cyclone (TC) genesis frequency (TCGF) has been documented to decrease or increase linearly in a changing climate. However, our numerical experiments show that the global TCGF exhibits a parabolic relation with spatio-uniform climate changes in sea surface temperature (SST) from −15 K to 5 K relative to the present climate, with the peak in the 5 K-cooler climate. The parabolic relation is found in all TC basins except the eastern North Pacific where TCGF keeps increasing with the changing climate. TCGF can be expressed as the product of the frequency of TC seeds and the TC survival rate (SR). Further analysis shows that this parabolic structure in the global TCGF depends on TC seeds rather than the TC SR. The TC SR exhibits an increasing trend with the SST increase, while TC seeds show a consistent change with TCGF, which might be linked to the changes in low-level relative humidity.

Plain Language Summary It is a hot-debated question as to how tropical cyclone (TC) genesis frequency (TCGF) would change under global warming. To address this problem, we examine the TCGF change in response to a simplified spatio-uniform change of sea surface temperature (SST) from −15 K to 5 K relative to the present climate. The global TCGF begins to increase with the global SST increase from −15 K, reaches peak in the 5 K-cooler climate, and subsequently decreases with further SST warming, forming a parabolic relation between the TCGF and the SST changes. Further, we find the parabolic relationship in all TC basins except the eastern North Pacific where the TCGF keeps increasing with SST changes. TCGF can be expressed as the product of the frequency of TC seeds and the TC survival rate (SR). Further analysis shows the TC SR cannot explain the global TCGF change, while the changes in frequency of TC seeds associated with the low-level relative humidity contribute to the parabolic change of TCGF.

1. Introduction

Among tropical cyclone (TC) metrics, the TC genesis frequency (TCGF) is perhaps the most poorly understood aspect under climate change (Sobel et al., 2021), which keeps an enduring enigma that frustrates climate scientists for decades yet unresolved (Emanuel, 2018). Therefore, unraveling how the TCGF changes is of great importance to the past, now and the future.

Satellite-based historic data have indicated an insignificant trend in the global TCGF, followed by a significant increase in the North Atlantic (NA) and a significant decrease in the western North Pacific (WNP) since 1990s (Klotzbach et al., 2022; Maue, 2011). However, there is low confidence as to how future TCGF would change under global warming (GW). Most previous studies based on high-resolution climate system models have shown a decreasing trend of TCGF under anthropogenic forcing scenarios (T. Knutson et al., 2020; Murakami et al., 2012; Sugi et al., 2009), while a portion of studies using dynamical downscaling method addressed an increasing trend (Emanuel, 2021a). This continuous debate limits the confidence for future projection of TCGF change.

The TCGF change is largely influenced by the projected sea surface temperature (SST) forcing (T. Knutson et al., 2020). Previous studies have revealed that the different SST warming patterns could lead to substantially distinct responses of TCGF over the globe, which is due to different responses of large-scale dynamic/thermodynamic conditions to the distinct zonal SST gradients associated with the different warming patterns (Murakami

Writing – review & editing: Ruifen Zhan

et al., 2012; J. Zhao, Zhan, & Wang, 2020). In addition, globally uniform SST change is also a notable factor for TCGF changes. A previous study revealed that TCGF becomes more in a 4 K-cooler climate compared with present-day (PD) climate, which indirectly supports the theory on the decrease of global TCGF under warming conditions (Sugi et al., 2015). However, it remains unclear whether the TCGF will further increase (decrease) with the global SST decreasing (increasing).

Recent studies proposed TCGF as the product of the TC seed frequency (TCSF) and the TC survival rate (SR; the ratio between TCGF and TC seeds or embryos) (Emanuel, 2022; Hsieh et al., 2020; Lee et al., 2020; Sugi et al., 2020; Vecchi et al., 2019; Yamada et al., 2021). Based on climate models, Vecchi et al. (2019) pointed out that global TCGF responds to low SR with an increase in TC seeds induced by GW and the less efficient development of these seeds into TCs. However, Sugi et al. (2020) drew a contrary conclusion that there would be a clear decrease in TC seeds under a warmer climate, which is likely to cause a decrease in relatively weak (category 2 or weaker) TCs. Yamada et al. (2021) further argued that the contributions of seed frequency and SR to TCGF varied among the models, with most models showing a decrease in seed frequency. Since TC seed and SR changes might play a key role in understanding future TCGF projections, the questions arise as to how TC seeds and the SR would change and which one contributes to TCGF change with the spatio-uniform SST warming or cooling.

This study seeks to understand how global TCGF responds to a changing climate. Based on a group of numerical experiments with a simplified spatio-uniform change of global SST from −15 K to 5 K relative to the PD climate, we found that the global TCGF exhibits a parabolic relation in the changing climate with the peak in the 5 K-cooler climate, and such a parabolic relation was attributed to the change in TC seed frequency.

2. Data and Methods

In this study, we mainly employed the High-Resolution Atmospheric Model (HiRAM) from Geophysical Fluid Dynamical Laboratory (GFDL) to conduct sensitive experiments. The HiRAM model has a horizontal resolution of approximately 50 km and 32 vertical levels, which can be used to explicitly extract TC-like vortices (M. Zhao et al., 2009, J. Zhao, Zhan, & Wang, 2020, J. Zhao, Zhan, Wang, et al., 2020). In the control (CTRL) run marked by 0 K, the HiRAM is integrated for 10 years from 1990 to 1999 using observationally monthly SST and sea ice content that is derived from the Met Office Hadley Centre datasets. Here, we spatio-uniformly decrease the observed PD SST from 1 K to 15 K, and increase the PD SST from 1 K to 5 K at an 1 K interval while other aerosols and anthropogenic greenhouse gases forcings are consistent with the CTRL run. So, the global SST anomalies in these experiments uniformly range from 15 K-cooler (−15 K run) to 5 K-warmer (5 K run) relative to the PD SST. The aim of these settings is to investigate how TCGF changes under a changing climate.

Here, the 6-hourly outputs from HiRAM, including sea level pressure, 850-hPa winds and vorticity, and the temperature averaged between 500-hPa and 300-hPa, are utilized to derive the TC vortices and seeds. The TC detection algorithm was downloaded from GFDL website (https://www.gfdl.noaa.gov/tstorms/), which matches with the HiRAM used in this study and has been widely used in previous studies (T. R. Knutson et al., 2013; M. Zhao et al., 2009). The basic extraction criteria and steps are as follows: First, there appears a low-pressure center on the ground. Considering that the TC intensity is initially weak, and the structure is asymmetrical, the ground isobars could not be closed. Second, for the vortex to reach a TC strength, the 850 hPa wind speed was not less than 17 m s^{-1} and the absolute value of the vorticity was greater than 5×10^{-5} s^{-1} at the same time. Third, the temperature in the range of 1,200 km in the TC center was higher than the temperature in the range of 1,200–2,400 km at 300–500 hPa to ensure a warm core structure. Finally, the TC lifespan should have been at least 1.5 days. The detection algorithm of TC seeds is similar to that of TCs but none of the thresholds for the intensity and life span are set. As a result, TC seeds have warm core structure and include embryo and incipient vortices of TCs. It should be mentioned that TC seed definition here is selected because the warm core structure is unique for TCs, which is also the first step determining whether an initial disturbance can develop into a TC.

The observational TCGF is derived from the International Best Track Archive for Climate Stewardship (IBTrACS; Knapp et al., 2010, 2018). The climatological mean of global TCGF is 85 in observation during 1990–1999. Here, we define the TC genesis location as the TC surface maximum wind speed equal to or larger than 35 knots (17 m s^{-1}) for the first time. The global TCGF in this study is defined as the TC genesis between 40°S and 40°S. The WNP covers the region (EQ–40°N, 100°E−180°); the eastern North Pacific (ENP) is the rest region of North

19448007, 2023, 9, Downloaded from https://agupubs.onlinelibrary.wiley.com/doi/10.1029/2023GL102879 by CochraneChina, Wiley Online Library on [13/11/2026]. See the Terms and Conditions (https://onlinelibrary.wiley.com/terms-and-conditions) on Wiley Online Library for rules of use; OA articles are governed by the applicable Creative Commons License

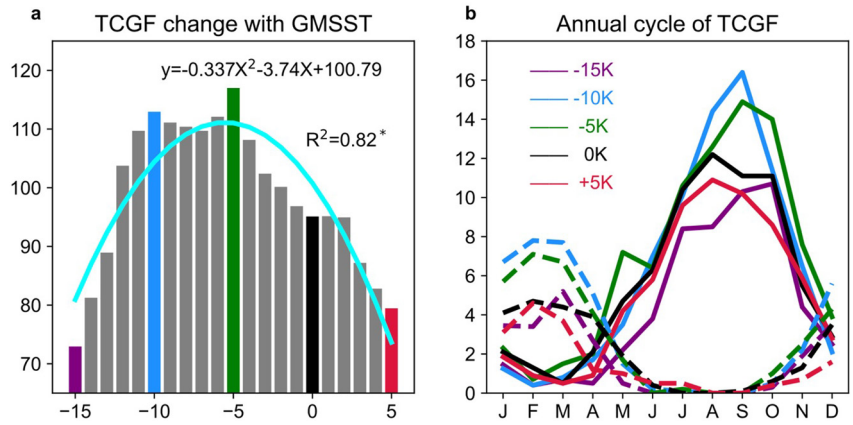


Figure 1. Global tropical cyclone genesis frequency (TCGF) changes in response to globally uniform warming or cooling. (a) Global TCGF change in response to spatio-uniform warming or cooling with the sea surface temperature (SST) changing from −15 K to 5 K at 1 K interval relative to the present-day (PD) climate; (b) seasonal cycle of Northern (solid) and Southern (dashed) Hemisphere TCGFs. In (a), the abscissa indicates the SST changing from −15 K to 5 K at 1 K interval relative to the PD climate. The black bars with the abscissa of "0" represent PD in the model; the red bars indicate 5 K-warmer compared with PD climate; the green, blue and purple bars stand for 5 K, 10 K, and 15 K-cooler, respectively. The cyan line is the polynomial fitting of TCGF changes with SST. The solid lines in (b) represent the Northern Hemisphere TCGF while the dashed lines are the Southern Hemisphere TCGF.

Pacific after removing WNP; the NA is defined as the region (EQ–30°N; 10°W–80°W), and the Southern Hemisphere (SH) ocean is the region (EQ–40°S, 40°E−180°). Note that in this study we did not consider the TCGF over the Indian Ocean due to the poor samples.

3. Results

Figure 1 shows the global TCGF change in response to spatio-uniform warming or cooling with the SST changing from −15 K to 5 K at 1 K interval relative to the PD climate (1990–1999). As expected, the global TCGF keeps decreasing when the global SST uniformly increases from 1 K to 5 K relative to the PD climate, consistent with most previous modeling results under GW (Chand et al., 2022; T. R. Knutson et al., 2015; Murakami et al., 2012; Sugi & Yoshimura, 2012). Similar to the work in a cooler climate by Sugi et al. (2015), the global TCGF starts to significantly increase when the global SST becomes cooler from −1 K to −5 K relative to the PD climate. However, when we further cool the global SST, the TCGF turns to reduce. Especially, such a reduction is robust when the global SST is about 10 K–15 K cooler than PD. This means that the relationship between the global TCGF and SST changes exhibits an approximately parabolic structure. We can directly fit a parabolic function $y = 0.337x^2 - 3.74x + 100.79$, demonstrating to be statistically significant in the parabolic fit with the fitting rate $R^2 = 0.82$. The annual cycle of global TCGF with 5 K intervals in response to spatio-uniform SST change is shown in Figure 1b. Generally, TCGF is higher at −5 K than at 0 K (−15 K and 5 K), and comparable with that at −10 K in both Hemispheres. It is worth noting that TCGF remains stable when the global SST increases from 1°C to 2°C, which could partially explain why we cannot detect a significant change in global TCGF from historical records (Emanuel, 2018; Sobel et al., 2021). Also, we note that the TCGF keeps relatively stable from −10 K to −6 K, indicating that the climate system has strong resilience.

Previous studies have shown the observed TCGF trend in the past half century is basin-dependent (Emanuel, 2018, 2021b; Sobel et al., 2021; Walsh et al., 2016; J. Zhao et al., 2018). Here, we further investigate the TCGF change under the changing climate for individual basins. We divide the globe into four subregions: the NA, the WNP, the ENP, and the SH, and the regional TCGF changes as a function of SST changes are shown in Figure 2. Similar to the global, the TCGF over the NA shows a significant parabolic relation with the uniform SST change with $R^2 = 0.89$. The NA TCGF reaches a maximum in the 5 K-cooler climate than the PD climate, whereas it starts to decrease when the global SST change departures from −5 K (Figure 2a). The WNP TCGF change also generally shows a parabolic relation ($R^2 = 0.75$) that the TCGF firstly increases from 32 at −15 K to the peak (about 43 at −5 K) and then gradually decreases to 31 with the global SST warming (Figure 2b). Similar to the NA and WNP, the SH TCGF also exhibits a significantly parabolic structure (Figure 2d). However, the

19448007, 2023, 9, Downloaded from https://agupubs.onlinelibrary.wiley.com/doi/10.1029/2023GL102879 by CochraneChina, Wiley Online Library on [13/11/2026]. See the Terms and Conditions (https://onlinelibrary.wiley.com/terms-and-conditions) on Wiley Online Library for rules of use; OA articles are governed by the applicable Creative Commons License

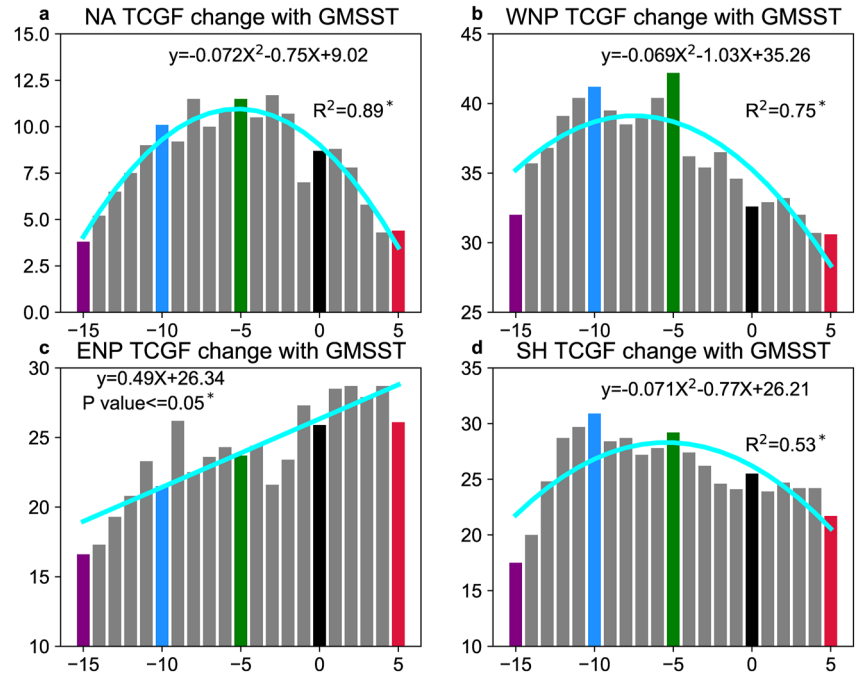


Figure 2. Tropical cyclone genesis frequency changes over individual basins in response to globally uniform warming or cooling. (a) The North Atlantic; (b) the western North Pacific; (c) the eastern North Pacific; and (d) the Southern Hemisphere. The abscissa indicates the global mean sea surface temperature (SST) changing from −15 K to 5 K at 1° interval relative to the present-day (PD) climate. The black bars with the abscissa of "0" represent PD in the model; the red bars indicate 5 K-warmer compared with PD climate; the green, blue and purple bars stand for 5 K, 10 K, and 15 K-cooler, respectively. The cyan line is the polynomial fitting of relative humidity changes with SST.

fitting rate R^2 is 0.53, much lower than that for the other two basins. In sharp contrast, over the ENP (Figure 2c), the TCGF in response to global SST changes displays a nearly linearly increasing trend, significant at a 95% confidence level, consistent with previous studies that the ENP TCGF remains increasing under the anthropogenic forcing (J. Zhao, Zhan, Wang, et al., 2020). However, it remains unclear whether this increasing trend would continue or turn to a decrease when the global SST further gets warmer. The above results suggest that the NA basin plays a more important role in contributing to the parabolic relation between the global TCGFs and the uniform SST changes, compared to the WNP and the SH.

To further understand the above relation between the global TCGF and the changing climate, we explore the responses of TC seed frequency and SR in the global to the global SST change, as shown in Figure 3. Similar to the TCGF change, the TCSF exhibits a significant parabolic relation with the changing SST with the high TCSF covering from −4 K to −12 K. In sharp contrast, the SR shows a significantly increasing trend (p value < 0.05) with a uniform increase in global SST (Figure 3b). It strongly suggests that the global TCGF in a changing climate is totally dependent on TC seeds rather than the SR, consistent with the results of most models (Yamada et al., 2021). It also suggests that GW always helps TC seeds more effectively develop into TCs, followed by an enhanced probability for more intense TCs in a warmer climate (T. R. Knutson et al., 2015). It also can be confirmed from the simulated TC intensity (Figure S1 in Supporting Information S1), although the resolution of HiRAM limited the number of intense TCs.

The formation of TC seeds is quite different from the physics of TC intensification (Emanuel, 2022). However, it remains unclear as to what controls the number of seeds up to now. TC is a vortex system with deep convection in the PD climate and a warmer scenario because the moisture supply is abundant from the ocean. But, the TC-like vortex could be drier, smaller, and shallower in the cooler climate (Figure S2 in Supporting Information S1, left panel). So, the low-level relative humidity (RH) could show substantial differences in triggering TC seeds in a changing climate. To test this hypothesis, Figure 4 shows low-level RH change integrated from 950 to 850 hPa over the individual basins in response to globally uniform warming or cooling, with the corresponding spatial distributions shown in Figure S3 in Supporting Information S1 and four-basin averaged

19448007, 2023, 9, Downloaded from https://agupubs.onlinelibrary.wiley.com/doi/10.1029/2023GL102879 by CochraneChina, Wiley Online Library on [13/11/2026]. See the Terms and Conditions (https://onlinelibrary.wiley.com/terms-and-conditions) on Wiley Online Library for rules of use; OA articles are governed by the applicable Creative Commons License

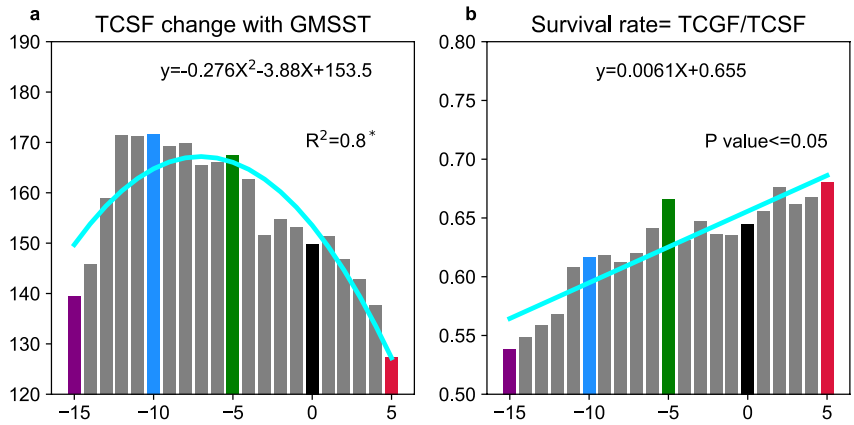


Figure 3. Changes in the global TC seed frequency (TCSF) and survival rate (SR) in response to globally uniform warming or cooling. (a) TCSF change; (b) SR defined as the ratio between tropical cyclone genesis frequency and TCSF. The abscissa indicates the sea surface temperature (SST) changing from −15 K to 5 K at 1° interval relative to the present-day (PD) climate. The black bars with the abscissa of "0" represent the PD climate in the model; the red bars indicate 5 K-warmer compared with the PD climate; the green, blue and purple bars stand for 5 K, 10 K, and 15 K-cooler, respectively. The cyan line is the polynomial fitting of relative humidity changes with SST.

low-level RH change in Figure S4 in Supporting Information S1. We can see that the low-level RH changes in a changing climate are highly consistent with the TCSF and TCGF changes (Figures 1 and 3), showing a parabolic relationship with global SST. In details, the RH changes over the WNP, NA and SH all show a parabolic relationship with the globally uniform SST changes. The RH reaches the maximum in a relatively cooler climate (about −5 K) whereas it decreases with the higher or lower SST. In sharp contrast, over the ENP the low-level RH keeps increasing with the SST changing from −15 K to 5 K, which is consistent with

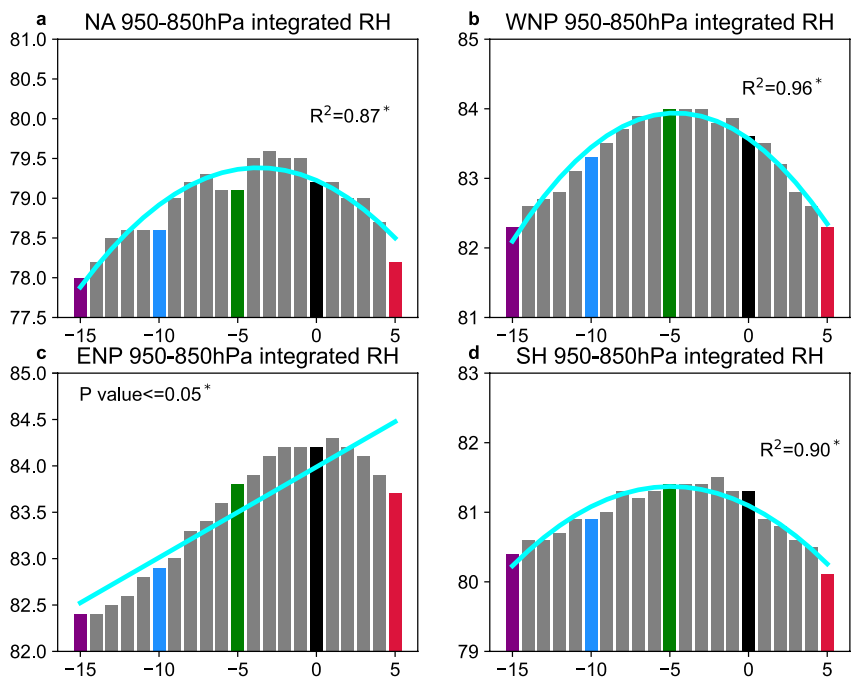


Figure 4. Low-level relative humidity (RH) change integrated from 950 hPa to 850 hPa over the individual basins in response to globally uniform warming or cooling. (a) The North Atlantic; (b) the western North Pacific; (c) the eastern North Pacific; and (d) the Southern Hemisphere. The abscissa indicates the sea surface temperature (SST) changing from −15 K to 5 K at 1° interval relative to the present-day (PD) climate. The black bars with the abscissa of "0" represent PD in the model; the red bars indicate 5 K-warmer compared with PD climate; the green, blue and purple bars stand for 5 K, 10 K, and 15 K-cooler, respectively. The cyan line is the polynomial fitting of RH changes with SST.

19448007, 2023, 9, Downloaded from https://agupubs.onlinelibrary.wiley.com/doi/10.1029/2023GL102879 by CochraneChina, Wiley Online Library on [13/11/2026]. See the Terms and Conditions (https://onlinelibrary.wiley.com/terms-and-conditions) on Wiley Online Library for rules of use; OA articles are governed by the applicable Creative Commons License

19448007, 2023, 9, Downloaded from https://agupubs.onlinelibrary.wiley.com/doi/10.1029/2023GL102879 by CochraneChina, Wiley Online Library on [13/11/2026]. See the Terms and Conditions (https://onlinelibrary.wiley.com/terms-and-conditions) on Wiley Online Library for rules of use; OA articles are governed by the applicable Creative Commons License

the increasing trend of ENP TCGF (Figure 2). Thus, we propose the hypothesis that the low-level RH could be responsible for the TC seed change in a changing climate. We also explored the saturation deficit (Emanuel et al., 2008) (Figure S5 in Supporting Information S1), which is important for TC genesis. Saturation deficit at 850 hPa (as well as 925 and 600 hPa; figure not shown) displays an increase in the 5 K-warmer climate relative to the PD climate. It indicates that the increased saturation deficit would suppress more TC geneses, consistent with previous studies (Emanuel et al., 2008). However, the saturation deficit keeps decreasing with the SST starting to reduce, which could not explain the parabolic relationship between TCGF and uniform SST changes. It is more likely that saturation deficit dominates the SR. However, these hypotheses need to be further tested in future.

4. Conclusion and Discussion

In this study, we examined the TCGF change in a changing climate, which has important implications for past and future climate changes. Consistent with previous studies, the modeled TCGF will decrease with the globally uniform SST changes from −5 K to 5 K relative to the PD climate. However, the TCGF will turn to increase with the SST changes from −15 K to −5 K, with the peak at −5 K. There is a significant parabolic relationship between the global TCGF and SST changes. This parabolic relationship is evident over the NA, the WNP and the SH. However, the ENP TCGF change is distinct with a nearly linearly increasing trend in response to the globally uniform SST change. Further analysis shows that this parabolic structure in the global TCGF depends on TC seeds rather than the SR. The former is consistent with the changes in low-level RH (which is better to represent the drier and shallower TCs in a cooler climate), while the latter shows a significant upward trend with the increase in global SST, which is consistent with the saturation deficit hypothesis.

It is interesting to see a peak between −10 K and −5 K (Figure 1). At present, there is not any theory that can well explain it. However, there are some clues to understanding this issue, TCs become weaker and weaker with the cooling of global mean SST (GMSST) (T. Knutson et al., 2020). This would lead to the reduction of TCGF when GMSST is extremely low, because the tropical disturbances may not be able to reach the TC intensity at these low SSTs. On the other hand, the increase of GMSST would increase the atmospheric static stability and then reduce time-mean upward mass flux (Sugi et al., 2012), which also would lead to the reduction of TCGF when SST is further high. Combining the above two clues, there must be an SST threshold, making the TCGF the most. It deserves future works based on very-high resolution models that can resolve realistic TC intensities.

This study shows the possible characteristics of TCGF change in response to spatio-uniform warming and cooling. However, the realistic SST warming pattern induced by the anthropogenic forcing is nonuniform (Seager et al., 2019; Xie, 2020; Xie et al., 2010). This nonuniform SST warming effect and relative contributions from the uniform and nonuniform SST warming to TCGF change will be discussed in our next work. Our experiments are idealized without considering the continents drifts and landcover area change, as well as many other settings. With these default settings, we are interested in another important problem. If the global SST keeps warming, for instance to 10 K warming, would the TCGF further keep decreasing? We also tested a simulation with 10 K warming and found that the TCGF does not decrease compared with the 5 K warming. So, the parabolic relationship between global TCGF and SST changes might be conditionally restricted. Finally, there is no existing theory to explain why the global TCGF reaches a maximum in 5 K-cooler climate relative to PD climate (Sugi et al., 2015; Walsh et al., 2016), which is an interesting scientific question and deserves further study in the future.

Data Availability Statement

The HIRAM model data used in this study can be downloaded from figshare website (https://doi.org/10.6084/m9.figshare.21928500.v1). The IBTrACS data (Knapp et al., 2010) is downloaded from https://doi.org/10.25921/82ty-9e16. The GFDL HIRAM C180 (M. Zhao et al., 2009) is downloaded from Geophysical Fluid Dynamics Laboratory website: https://www.gfdl.noaa.gov/hiram-quickstart. The TC detection algorithm (M. Zhao et al., 2009) is downloaded from Geophysical Fluid Dynamics Laboratory website: https://www.gfdl.noaa.gov/tstorms/. Calculations and Figures were made with Python v3.9.12 (Van Rossum & Drake, 2009) available under https://www.anaconda.com.

Acknowledgments
We are grateful to two anonymous reviewers for their insightful and valuable feedback that improved the quality of the manuscript. This work is jointly supported by the National Natural Science Foundation of China (Grants 42288101, 42105022, 42075015, 42075003, 42105042).

References

Chand, S. S., Walsh, K. J. E., Camargo, S. J., Kossin, J. P., Tory, K. J., Wehner, M. F., et al. (2022). Declining tropical cyclone frequency under global warming. *Nature Climate Change*, *12*(7), 655–661. https://doi.org/10.1038/s41558-022-01388-4

Emanuel, K. (2018). 100 years of progress in tropical cyclone research. *Meteorological Monographs*, *59*, 15.1–15.68. https://doi.org/10.1175/AMSMONOGRAPHS-D-18-0016.1

Emanuel, K. (2021a). Atlantic tropical cyclones downscaled from climate reanalyses show increasing activity over past 150 years. *Nature Communications*, *12*(1), 7027. https://doi.org/10.1038/s41467-021-27364-8

Emanuel, K. (2021b). Response of global tropical cyclone activity to increasing CO_2: Results from downscaling CMIP6 models. *Journal of Climate*, *34*(1), 57–70. https://doi.org/10.1175/JCLI-D-20-0367.1

Emanuel, K. (2022). Tropical cyclone seeds, transition probabilities, and genesis. *Journal of Climate*, *35*(11), 3557–3566. https://doi.org/10.1175/JCLI-D-21-0922.1

Emanuel, K., Sundararajan, R., & Williams, J. (2008). Hurricanes and global warming: Results from downscaling IPCC AR4 simulations. *Bulletin of the American Meteorological Society*, *89*(3), 347–368. https://doi.org/10.1175/BAMS-89-3-347

Hsieh, T.-L., Vecchi, G. A., Yang, W., Held, I. M., & Garner, S. T. (2020). Large-scale control on the frequency of tropical cyclones and seeds: A consistent relationship across a hierarchy of global atmospheric models. *Climate Dynamics*, *55*(11–12), 3177–3196. https://doi.org/10.1007/s00382-020-05446-5

Klotzbach, P. J., Wood, K. M., Schreck, C. J., Bowen, S. G., Patricola, C. M., & Bell, M. M. (2022). Trends in global tropical cyclone activity: 1990–2021. *Geophysical Research Letters*, *49*(6). https://doi.org/10.1029/2021GL095774

Knapp, K. R., Diamond, H. J., Kossin, J. P., Kruk, M. C., & Schreck, C. J. (2018). *International best track archive for climate stewardship (IBTrACS) project, version 4* [WP, NP, NA, SI, NI, SP]. NOAA/National Centers for Environmental Information. https://doi.org/10.25921/82ty-9e16

Knapp, K. R., Kruk, M. C., Levinson, D. H., Diamond, H. J., & Neumann, C. J. (2010). The international best track archive for climate stewardship (IBTrACS): Unifying tropical cyclone data. *Bulletin of the American Meteorological Society*, *91*(3), 363–376. https://doi.org/10.1175/2009BAMS2755.1

Knutson, T., Camargo, S. J., Chan, J. C. L., Emanuel, K., Ho, C.-H., Kossin, J., et al. (2020). Tropical cyclones and climate change assessment: Part II: Projected response to anthropogenic warming. *Bulletin of the American Meteorological Society*, *101*(3), E303–E322. https://doi.org/10.1175/BAMS-D-18-0194.1

Knutson, T. R., Sirutis, J. J., Gabriel, A. V., Garner, S., Zhao, M., Kim, H. S., et al. (2013). Dynamical downscaling projections of twenty-first-century Atlantic hurricane activity: CMIP3 and CMIP5 model-based scenarios. *Journal of Climate*, *26*(17), 6591–6617. https://doi.org/10.1175/JCLI-D-12-00539.1

Knutson, T. R., Sirutis, J. J., Zhao, M., Tuleya, R. E., Bender, M., Vecchi, G. A., et al. (2015). Global projections of intense tropical cyclone activity for the late twenty-first century from dynamical downscaling of CMIP5/RCP4.5 scenarios. *Journal of Climate*, *28*(18), 7203–7224. https://doi.org/10.1175/JCLI-D-15-0129.1

Lee, C.-Y., Camargo, S. J., Sobel, A. H., & Tippett, M. K. (2020). Statistical–dynamical downscaling projections of tropical cyclone activity in a warming climate: Two diverging genesis scenarios. *Journal of Climate*, *33*(11), 4815–4834. https://doi.org/10.1175/JCLI-D-19-0452.1

Maue, R. N. (2011). Recent historically low global tropical cyclone activity. *Geophysical Research Letters*, *38*(14). https://doi.org/10.1029/2011GL047711

Murakami, H., Wang, Y., Yoshimura, H., Mizuta, R., Sugi, M., Shindo, E., et al. (2012). Future changes in tropical cyclone activity projected by the new high-resolution MRI-AGCM. *Journal of Climate*, *25*(9), 3237–3260. https://doi.org/10.1175/JCLI-D-11-00415.1

Seager, R., Cane, M., Henderson, N., Lee, D.-E., Abernathey, R., & Zhang, H. (2019). Strengthening tropical Pacific zonal sea surface temperature gradient consistent with rising greenhouse gases. *Nature Climate Change*, *9*(7), 517–522. https://doi.org/10.1038/s41558-019-0505-x

Sobel, A. H., Wing, A. A., Camargo, S. J., Patricola, C. M., Vecchi, G. A., Lee, C., & Tippett, M. K. (2021). Tropical cyclone frequency. *Earth's Future*, *9*(12). https://doi.org/10.1029/2021EF002275

Sugi, M., Murakami, H., & Yoshimura, J. (2009). A reduction in global tropical cyclone frequency due to global warming. *SOLA*, *5*, 164–167. https://doi.org/10.2151/sola.2009-042

Sugi, M., Murakami, H., & Yoshimura, J. (2012). On the mechanism of tropical cyclone frequency changes due to global warming. *Journal of the Meteorological Society*, *90A*(0), 397–408. https://doi.org/10.2151/JMSJ.2012-A24

Sugi, M., Yamada, Y., Yoshida, K., Mizuta, R., Nakano, M., Kodama, C., & Satoh, M. (2020). Future changes in the global frequency of tropical cyclone seeds. *SOLA*, *16*(0), 70–74. https://doi.org/10.2151/sola.2020-012

Sugi, M., Yoshida, K., & Murakami, H. (2015). More tropical cyclones in a cooler climate? *Geophysical Research Letters*, *42*(16), 6780–6784. https://doi.org/10.1002/2015GL064929

Sugi, M., & Yoshimura, J. (2012). Decreasing trend of tropical cyclone frequency in 228-year high-resolution AGCM simulations. *Geophysical Research Letters*, *39*(19). https://doi.org/10.1029/2012GL053360

Van Rossum, G., & Drake, F. L. (2009). *Python 3 reference manual*. CreateSpace. Retrieved from https://docs.python.org/3.9/

Vecchi, G. A., Delworth, T. L., Murakami, H., Underwood, S. D., Wittenberg, A. T., Zeng, F., et al. (2019). Tropical cyclone sensitivities to CO_2 doubling: Roles of atmospheric resolution, synoptic variability and background climate changes. *Climate Dynamics*, *53*(9–10), 5999–6033. https://doi.org/10.1007/s00382-019-04913-y

Walsh, K. J. E., McBride, J. L., Klotzbach, P. J., Balachandran, S., Camargo, S. J., Holland, G., et al. (2016). Tropical cyclones and climate change: Tropical cyclones and climate change. *Wiley Interdisciplinary Reviews: Climate Change*, *7*(1), 65–89. https://doi.org/10.1002/wcc.371

Xie, S.-P. (2020). Ocean warming pattern effect on global and regional climate change. *AGU Advances*, *1*(1). https://doi.org/10.1029/2019AV000130

Xie, S.-P., Deser, C., Vecchi, G. A., Ma, J., Teng, H., & Wittenberg, A. T. (2010). Global warming pattern formation: Sea surface temperature and rainfall. *Journal of Climate*, *23*(4), 966–986. https://doi.org/10.1175/2009JCLI3329.1

Yamada, Y., Kodama, C., Satoh, M., Sugi, M., Roberts, M. J., Mizuta, R., et al. (2021). Evaluation of the contribution of tropical cyclone seeds to changes in tropical cyclone frequency due to global warming in high-resolution multi-model ensemble simulations. *Progress in Earth and Planetary Science*, *8*(1), 11. https://doi.org/10.1186/s40645-020-00397-1

Zhao, J., Zhan, R., & Wang, Y. (2020). Different responses of tropical cyclone tracks over the western North Pacific and North Atlantic to two distinct SST warming patterns. *Geophysical Research Letters*, *47*(7), e2019GL086923. https://doi.org/10.1029/2019GL086923

19448007, 2023, 9, Downloaded from https://agupubs.onlinelibrary.wiley.com/doi/10.1029/2023GL102879 by CochraneChina, Wiley Online Library on [13/11/2026]. See the Terms and Conditions (https://onlinelibrary.wiley.com/terms-and-conditions) on Wiley Online Library for rules of use; OA articles are governed by the applicable Creative Commons License

Zhao, J., Zhan, R., Wang, Y., Xie, S.-P., & Wu, Q. (2020). Untangling impacts of global warming and Interdecadal Pacific Oscillation on long-term variability of North Pacific tropical cyclone track density. *Science Advances*, *6*(41), eaba6813. https://doi.org/10.1126/sciadv.aba6813

Zhao, J., Zhan, R., Wang, Y., & Xu, H. (2018). Contribution of Interdecadal Pacific Oscillation to the recent abrupt decrease in tropical cyclone genesis frequency over the western North Pacific since 1998. *Journal of Climate*, *31*(20), 8211–8224. https://doi.org/10.1175/JCLI-D-18-0202.1

Zhao, M., Held, I. M., Lin, S.-J., & Vecchi, G. A. (2009). Simulations of global hurricane climatology, interannual variability, and response to global warming using a 50-km resolution GCM. *Journal of Climate*, *22*(24), 6653–6678. https://doi.org/10.1175/2009JCLI3049.1

19448007, 2023, 9, Downloaded from https://agupubs.onlinelibrary.wiley.com/doi/10.1029/2023GL102879 by CochraneChina, Wiley Online Library on [13/11/2026]. See the Terms and Conditions (https://onlinelibrary.wiley.com/terms-and-conditions) on Wiley Online Library for rules of use; OA articles are governed by the applicable Creative Commons License